Discovery of an intrinsic tenase complex inhibitor: Pure nonasaccharide from fucosylated glycosaminoglycan

Longyan Zhao[a,b,1], Mingyi Wu[a,1], Chuang Xiao[a,b], Lian Yang[a], Lutan Zhou[a,b], Na Gao[a,b], Zi Li[a], Jun Chen[a], Jianchao Chen[a], Jikai Liu[a,c,2], Hongbo Qin[a,2], and Jinhua Zhao[a,2]

[a]State Key Laboratory of Phytochemistry and Plant Resources in West China, Kunming Institute of Botany, Chinese Academy of Sciences, Kunming, Yunnan 650201, China; [b]University of Chinese Academy of Sciences, Beijing 100049, China; and [c]School of Pharmaceutical Sciences, South-Central University for Nationalities, Wuhan 430074, China

Edited by Jerrold Meinwald, Cornell University, Ithaca, NY, and approved May 21, 2015 (received for review March 2, 2015)

Selective inhibition of the intrinsic coagulation pathway is a promising strategy for developing safer anticoagulants that do not cause serious bleeding. Intrinsic tenase, the final and rate-limiting enzyme complex in the intrinsic coagulation pathway, is an attractive but less explored target for anticoagulants due to the lack of a pure selective inhibitor. Fucosylated glycosaminoglycan (FG), which has a distinct but complicated and ill-defined structure, is a potent natural anticoagulant with nonselective and adverse activities. Herein we present a range of oligosaccharides prepared via the deacetylation–deaminative cleavage of FG. Analysis of these purified oligosaccharides reveals the precise structure of FG. Among these fragments, nonasaccharide is the minimum fragment that retains the potent selective inhibition of the intrinsic tenase while avoiding the adverse effects of native FG. In vivo, the nonasaccharide shows 97% inhibition of venous thrombus at a dose of 10 mg/kg in rats and has no obvious bleeding risk. This nonasaccharide may therefore serve as a novel promising anticoagulant.

anticoagulant | inhibitors | oligosaccharides | carbohydrates | drug discovery

Thrombotic disease is seriously harmful to human health and is one of the major causes of death in modern society (1). Despite their long-term and widespread use as anticoagulants, heparin, low–molecular-weight heparin (LMWH), and coumarins still have a major unresolved issue: the risk of serious bleeding during therapy (1–3). It is generally recognized that the risk of bleeding associated with these agents is related to the nonselectivity of their anticoagulant activity. Therefore, selective inhibitors of human factor Xa (FXa) and thrombin (FIIa), such as dabigatran, rivaroxaban, and apixaban, which have predictable pharmacokinetics, have recently been developed; however, these agents have not effectively reduced the risk of bleeding in clinical applications (4–7).

Components of the intrinsic coagulation pathway are promising targets for antithrombotic therapy because they are important for thrombosis but are not required for hemostasis (1, 8). The development of new anticoagulant agents that inhibit components of the intrinsic pathway and that have a lower risk of causing bleeding has thus become a research focus (9–11). Factor IXa (FIXa), a serine protease, and factor VIIIa (FVIIIa), a protein cofactor, form a Ca^{2+}- and phospholipid surface-dependent complex referred to as the intrinsic tenase complex, which efficiently converts zymogen factor X (FX) to FXa (1, 12, 13). Because the intrinsic tenase is the final and rate-limiting enzyme complex in the intrinsic pathway, the development of inhibitors of this enzyme complex is important for meeting clinical demands (1). However, limited progress has been achieved due to the unavailability of selective inhibitors with well-defined structures.

Fucosylated glycosaminoglycan (FG; **1** in Fig. 1), which is a complex acidic polysaccharide isolated from sea cucumber, has recently attracted considerable attention because of its various bioactivities (14). Notably, FG has potent anticoagulant and antithrombotic activities due to its inhibition of the intrinsic tenase (15–17). However, the native polysaccharide has side effects such as factor XII (FXII) activation, platelet aggregation, and serious bleeding (18). Nowadays, depolymerization is considered to be an effective method for reducing these adverse effects (19). For over 30 y since its discovery the detailed structures of native FG and its depolymerized products have not been elucidated, because these polysaccharides are heterogeneous, namely they are mixtures of isomers with different molecular weights, and because limitations exist in the available strategies for analyzing such molecules (17, 20). For example, although it is assumed that a single fucose (Fuc) is linked to the C-3 position of glucuronic acid (GlcA) via an α-glycosidic bond, there is no direct evidence excluding the possibility that Fuc may be linked to the C-4 and C-6 positions of *N*-acetylgalactosamine (GalNAc) and that the Fuc side chain may exist as a di- or trisaccharide side chain (14, 21–24). Because the polydisperse and structurally ambiguous native FG and its ill-defined depolymerized products are not suitable for the precise evaluation of their structure–activity relationships, in general, the purification of FG-derived fragments is crucial for probing these structure–activity relationships with regard to the inhibition of the intrinsic tenase and for elucidating the detailed structure of FG. Detailed knowledge of the structures of fragments and of the native form of FG is also necessary for developing a clinically effective inhibitor of the intrinsic tenase that has fewer side effects. In this work, we prepared a class of homogeneous oligosaccharides using our newly developed selective depolymerization method. Analysis of these oligosaccharides revealed the precise structure of FG. To our delight, some of these oligosaccharides have potent anticoagulant activity by strongly and selectively inhibiting the intrinsic tenase while avoiding such side effects as FXII activation

Significance

Selective inhibition of the intrinsic coagulation pathway is a promising strategy for developing safer anticoagulants without serious bleeding consequences. We prepared and identified a series of oligosaccharides as inhibitors of the intrinsic tenase, which is the final and rate-limiting enzyme complex in the intrinsic coagulation pathway and is an attractive but less explored target for anticoagulants due to the lack of a pure selective inhibitor. Analysis of these purified oligosaccharides reveals the precise structure of fucosylated glycosaminoglycan. Among these oligosaccharides, nonasaccharide is the minimum fragment that retains potent anticoagulant activity by selective inhibition of the intrinsic tenase while avoiding adverse effects and, thus, it may pave the way for the development of better treatments for thromboembolic diseases.

Author contributions: J.L., H.Q., and J.Z. designed research; L. Zhao, M.W., C.X., L.Y., L. Zhou, N.G., Z.L., Jun Chen, and Jianchao Chen performed research; L. Zhao, M.W., J.L., H.Q., and J.Z. analyzed data; and L. Zhao, M.W., H.Q., and J.Z. wrote the paper.

The authors declare no conflict of interest.

This article is a PNAS Direct Submission.

[1]L.Z. and M.W. contributed equally to this work.

[2]To whom correspondence may be addressed. Email: jkliu@mail.kib.ac.cn, qinhongbo@mail.kib.ac.cn, or zhaojinhua@mail.kib.ac.cn.

This article contains supporting information online at www.pnas.org/lookup/suppl/doi:10.1073/pnas.1504229112/-/DCSupplemental.

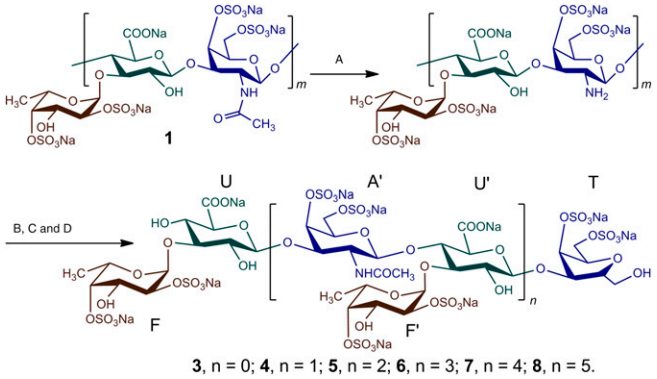

Fig. 1. Preparation of FG-derived oligosaccharides. The purified FG (i.e., **1**) was N-deacetylated with hydrazine hydrate (*A*) (yield 95%). The N-deacetylated **1** was then cleaved with nitrous acid (*B*), reduced with $NaBH_4$ (*C*), dialyzed, lyophilized to prepare **2** (yield 80%), and then fractionated by GPC (*D*) to obtain the pure oligosaccharides **3**–**8** (n = 0–5).

and platelet aggregation. Furthermore, we found that nonasaccharide is the minimum structural unit responsible for the selective inhibition of the intrinsic tenase, and that nonasaccharide strongly inhibits venous thrombus formation without bleeding consequences.

Results

Pure Oligosaccharides of FG Are Obtained Using a Selective Depolymerization Method and Gel Permeation Chromatography. **1** was isolated and purified from the sea cucumber *Stichopus variegatus* (Figs. 1 and 2*A*). Structural analysis of **1** was performed as described previously (21–23). The results of the physicochemical analysis showed that **1** and **2** are composed of the three monosaccharides GlcA, GalNAc, and Fuc and sulfate esters in a ratio of ~1:1:1:4.

To prepare pure fragments of FG, a key step is to establish a glucosidic bond-selective depolymerization method. To date, there have been no reports on the acquisition of pure fragments of FG using known depolymerization methods such as free-radical depolymerization and photochemical depolymerization (20, 25). Such depolymerization methods are nonselective and result in excess fragments that render further purification difficult. Recently, we established a partial N-deacetylation–deaminative cleavage method (17) that may be functional group-selective with no obvious sulfate group or Fuc branch loss. Thus, this method is useful for preparing pure fragments of FG. In this study, we prepared depolymerized **1** (i.e., **2** in Figs. 1 and 2*B*), which is a mixture of fragments (molecular mass 5.4 kDa), using high-performance gel permeation chromatography (GPC).

The fractionation of **2** using GPC with Bio-Gel P6 and P10 columns combined with analysis using a Superdex Peptide 10/300 GL column afforded a range of homogeneous oligosaccharides (Fig. 2 *C* and *D*), which were identified as tri, hexa-, nona-, dodeca-, pentadeca-, and octadecasaccharides based on the ratio of the peak area of the anomeric proton peak of Fuc residues at different positions of their chains in their ^{1}H NMR spectra. The desalted pure oligosaccharides were water-soluble white powders (HPLC purity >99.9%) (**3**–**8** in Fig. 2*D*).

Characterization of Oligosaccharides Results in Elucidation of the Precise Structure of FG. As shown in the NMR spectra of **1** (*SI Appendix*, Fig. S2), although signals of monosaccharide residues can be roughly assigned, they give overlapping spectra with broad signals, thus hindering elucidation of the precise structures. It is particularly difficult to identify the connection patterns of both the backbone and the Fuc side chains. The NMR spectra of **2** are clearer than those of **1**; however, the signals are still significantly overlapped, as expected for its high molecular mass and mixtures of isomers (*SI Appendix*, Fig. S2). We therefore sought to decipher the structure of **1** by analyzing its depolymerized and purified fragments using a bottom-up approach similar to a jigsaw puzzle (26).

The NMR spectra clearly show that **3** is a trisaccharide (Fig. 3 *A*, *C*, and *E* and *SI Appendix*, Figs. S4–S7). The complete assignment of its peaks is shown in *SI Appendix*, Table S1. The H-1 proton of each sugar can be assigned to 5.56, 4.53, and 3.68–3.79 ppm for Fuc, GlcA, and 2,5-anhydro-D-talitol (anTal-ol), respectively. Their C-1 signals are 99.9, 104.4, and 63.8 ppm, respectively (Fig. 3 *A* and *C*). The locations of the attached sulfates on each sugar residue were deduced from the downfield shifts of protons on attached carbons caused by the sulfation compared with corresponding unsubstituted monosaccharide, which shows that anTal-ol is sulfated at both the C-4 and C-6 positions and that Fuc is sulfated at both the C-2 and C-4 positions. Additionally, the heteronuclear single quantum correlation (HSQC) spectrum (*SI Appendix*, Fig. S7*A*) confirmed these sulfated positions on Fuc and anTal-ol. The small H-H coupling constants (3.8 Hz) indicate the presence of an α-linkage between Fuc and GlcA, and the larger H-H coupling constants (8.4 Hz) indicate the presence of a β-linkage between GlcA and anTal-ol. Further analysis using rotating frame overhauser effect spectroscopy (ROESY) and heteronuclear multiple bond correlation (HMBC) (Fig. 3*E* and *SI Appendix*, Fig. S6*A*) confirmed that the C-1 position of Fuc is connected to the C-3 position of GlcA and that a similar (C-1–C-3) connection occurs between GlcA and anTal-ol. Therefore, **3** is determined to be the trisaccharide L-Fuc_{2S4S}-α1,3-D-GlcA-β1,3-D-anTal-ol_{4S6S}. In addition, electrospray ionization quadrupole time-of-flight mass spectrometry (ESI-Q-TOF-MS) analysis revealed an m/z of 892.8954 for $[M\text{-}Na]^-$, which is identical to the calculated value of 892.9057, confirming that the molecular formula of **3** is $C_{18}H_{26}O_{27}S_4Na_5$ (Fig. 3*G*).

Compound **4** presents chemical signals from Fuc (*SI Appendix*, Table S1), GlcA, and anTal-ol similar to those from **3** during 1D and 2D NMR analyses. The ^{1}H NMR spectrum of **4** shows additional H-1 peaks of GlcA, Fuc, and GalNAc residues, which can be easily assigned according to correlation spectroscopy (COSY). Similarly, compared with that of **3**, the ^{13}C NMR spectrum of **4**

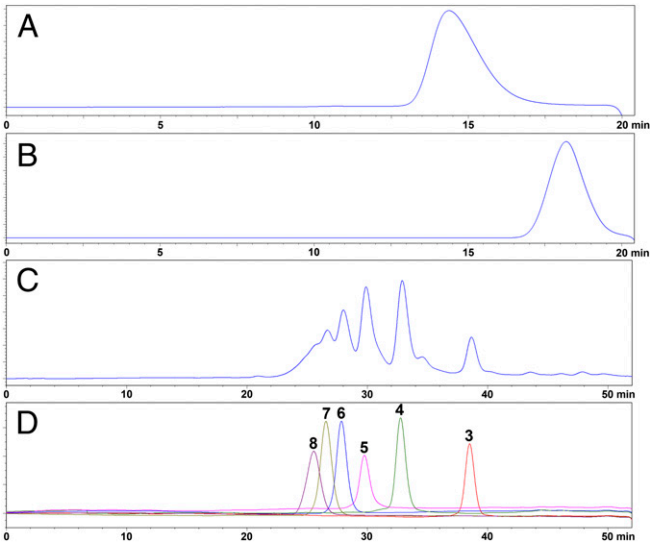

Fig. 2. HPLC profiles of **1**–**8**. (*A* and *B*) HPLC profiles of **1** and **2**, respectively, determined using a Shodex OHpak SB-804 HQ column (8 mm × 300 mm). Aliquots of 50 μL of 1–2 mg/mL samples were analyzed on an Agilent Technologies 1200 series apparatus with 0.1 M NaCl as the eluent at a flow rate of 0.5 mL/min. The analysis was monitored using a differential refraction detector. (*C* and *D*) HPLC profiles of **2** and **3**–**8**, respectively, analyzed using a Superdex Peptide 10/300 GL column (10 mm × 300 mm). Aliquots (50–100 μL) of 2–4 mg/mL oligosaccharide samples were size-fractionated using 0.2 M NaCl as the eluent at a flow rate of 0.4 mL/min.

BIOCHEMISTRY

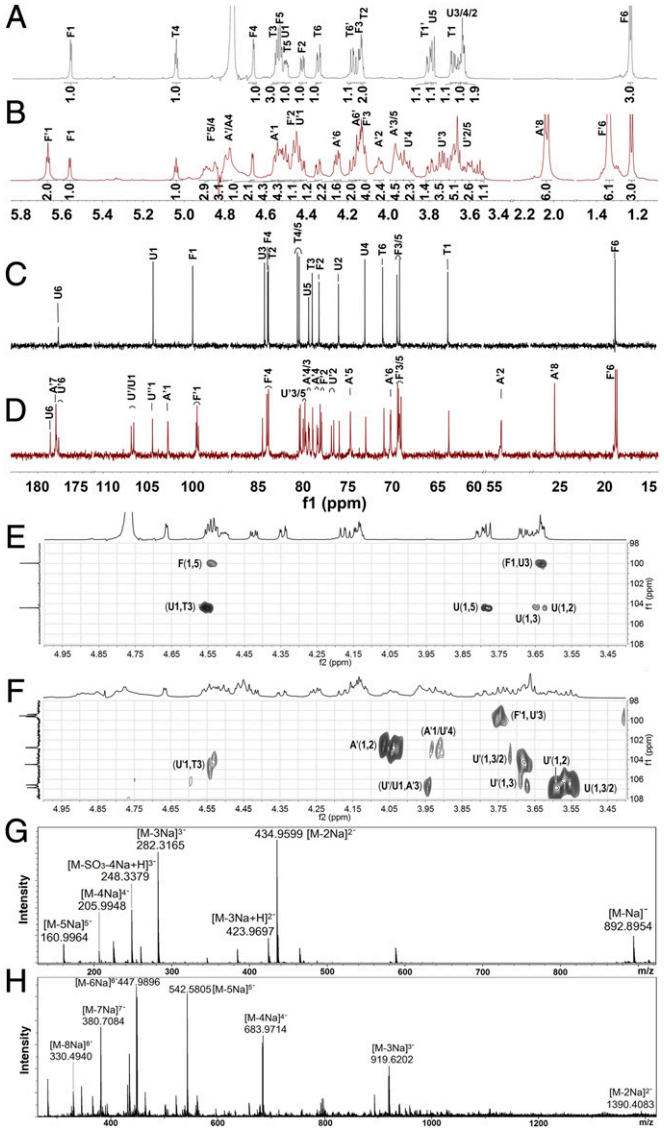

Fig. 3. ^{1}H (*A* and *B*), ^{13}C (*C* and *D*), partial ^{1}H-^{13}C HMBC (*E* and *F*), and Q-TOF spectra (*G* and *H*) of compounds **3** (*A*, *C*, *E*, and *G*) and **5** (*B*, *D*, *F*, and *H*). Labels are the same as those in Fig. 1.

shows additional terminal C signals, which can be further assigned by HSQC (*SI Appendix*, Fig. S7*B*). The sites of sulfation are at the C-2 and C-4 positions of Fuc and at the C-4 and C-6 positions of GalNAc and anTal-ol. The ROESY and HMBC spectra show that the Fucs in **4** are linked through C-1 to C-3 of GlcAs, GalNAc is linked through C-1 to C-4 of GlcA, and GlcAs are linked through C-1 to C-3 of GalNAc and anTal-ol. α- or β-linkages can also be determined by the H-H or C-H coupling constants. The ESI-Q-TOF-MS of **4** afforded a mass-to-charge value of 912.4039, which is consistent with $[M\text{-}2Na]^{2-}$ (calculated *m/z* 912.4112), indicating a molecular formula of $C_{38}H_{51}O_{54}N_1S_8Na_{10}$ (*SI Appendix*, Fig. S8). Further assignments (*SI Appendix*, Table S1) indicate that **4** possesses the structure L-Fuc$_{2S4S}$-α1,3-D-GlcA-β1,3-D-GalNAc$_{4S6S}$-β1,4-[L-Fuc$_{2S4S}$-α1,3-]D-GlcA-β1,3-D-anTal-ol$_{4S6S}$. Clearly, **4** contains an additional trisaccharide that is β1,4–linked to the GlcA of **3**.

The structure of **5** was confirmed using the same methods as for **3** and **4**. ^{1}H and ^{13}C NMR signals (Fig. 3 *B* and *D* and *SI Appendix*, Table S2) can be assigned by 2D NMR (Fig. 3*F* and *SI Appendix*, Figs. S4*B*, S6*B*, and S7*C*). **5** had the characteristic mass-to-charge peaks of $[M\text{-}2Na]^{2-}$ (i.e., 1390.4083, calculated *m/z* 1389.6393), $[M\text{-}3Na]^{3-}$ (i.e., 919.6202, calculated *m/z* 918.9129), and others in its ESI-Q-TOF-MS spectrum (Fig. 3*H*). ESI-Q-TOF-MS and NMR analyses suggest that **5** possesses the structure L-Fuc$_{2S4S}$-α1,3-D-GlcA-β1,3-{D-GalNAc$_{4S6S}$-β1,4-(L-Fuc$_{2S4S}$-α1,3-)D-GlcA-β1,3-}$_2$-D-anTal-ol$_{4S6S}$, in which another trisaccharide is linked to hexosaccharide **4**. These results suggest that the additional trisaccharide may exist in **1** as a repeating unit.

The spectra of **6**–**8** indicate that they are dodeca-, pentadeca-, and octadecasaccharides, respectively (*SI Appendix*, Figs. S3–S5 and Table S2). With the exception of the trisaccharide containing an anTal-ol produced by the deaminative cleavage at the reducing end in **6**–**8**, the other sequence of these oligosaccharides is constituted by the repeating trisaccharide unit -{(L-Fuc-α1,3-)D-GlcA-β1,3-D-GalNAc-β1,4-}-, where Fuc side chains and GalNAc residues are primarily Fuc$_{2S4S}$ and GalNAc$_{4S6S}$, respectively.

Overall, the Fuc side chain in **3**–**8** only exists as a monosaccharide and only attaches to GlcA through an α1,3-linkage, a di- or trisaccharide side chain is absent, and no Fuc side chain links to GalNAc (or anTal-ol). Considering that anTal-ols are produced by the deaminative cleavage and that the ratios of monosaccharides and sulfate esters in **3**–**8** are the same as that in native compound **1**, we conclude that the deacetylation–deaminative cleavage is highly dependent on the functional group and does not affect the substituted Fuc or sulfate. Based on the characteristic structures of **3**–**8**, the structure of **1** can be rationally deduced to be composed of repeating units of D-GlcA-β1,3-D-GalNAc-β1,4- in the backbone and a monosaccharide Fuc side chain that is connected to GlcA of the backbone through an α1,3-glycosidic bond.

Further analysis of the NMR spectra indicates that very few of the Fuc$_{4S}$ and Fuc$_{3S4S}$ residues that occur in native **1** are also α1,3-linked to GlcA (*SI Appendix*, Fig. S2). These Fuc residues also exist in the pure oligosaccharides (**3**–**8**) in the same glycosidic linkage. This result further suggests that deacetylation–deaminative cleavage is mild and highly selective, which assures the integrity of the repeating unit. Thus, this method may be applicable for analyzing the structures of other glycosaminoglycans, including FG from other sea cucumber species (19–23).

Compounds 5–8 Exhibit Strong Anticoagulant Activities by Selective Inhibition of the Human Intrinsic Tenase. The anticoagulant activities of **1**–**8** were evaluated using the activated partial thromboplastin time (APTT), prothrombin time (PT), and thrombin time (TT) of plasma clotting assays (Table 1), which are used to determine the ability to inhibit blood clotting through the intrinsic, extrinsic, and common pathways of the coagulation cascade, respectively (27). Concentrations between 1.8 and 14.5 μg/mL of **1**, **2**, and **5**–**8** are required to double the APTT, indicating that these compounds have potent intrinsic anticoagulant activities that are more potent than or similar to that of LMWH. Notably, **3** and **4** have weak or negligible effects on APTT. Regarding PT and TT, no significant influences were observed for **2**–**8** at concentrations as high as 128 μg/mL, thus indicating that these compounds have no or little effect on the extrinsic and common coagulation pathways.

Furthermore, **1**, **2**, and **5**–**8** potently inhibit the intrinsic tenase, and do not exhibit inhibition of FIXa in the absence or presence of AT (Fig. 4 and *SI Appendix*, Fig. S10). Additionally, they have no antithrombin (AT)-dependent or AT-independent inhibition of factor VIIa (FVIIa), FXa, factor XIa (FXIa), or factor XIIa (FXIIa). **3** and **4** exhibit no inhibition of the intrinsic tenase or these factors (Table 1 and *SI Appendix*, Figs. S9 and S10). **1** exhibits strong AT-dependent anti-FIIa activity. In contrast, this effect was not observed for **2**–**7** at concentrations as high as 2,000 ng/mL (Table 1 and *SI Appendix*, Fig. S9*B*). Remarkably, **5**–**8** exhibit considerably stronger anti-tenase activity, more than 1,000-fold higher than anti-FXa activity and 100-fold higher than anti-FIIa in the presence of AT, indicating that their anticoagulant mechanisms are significantly different from those of heparin-like drugs. Additionally, **5**–**8** exhibit some heparin cofactor

II (HCII)-dependent FIIa inhibition; however, their potency (400–950 ng/mL) is considerably weaker than that for intrinsic tenase inhibition (*SI Appendix*, Fig. S9*C*).

Compounds 3–7 Do Not Show the FXII Activation and Platelet Aggregation Exhibited by Native FG. As described above, **1** exhibited some FXII activation; oversulfated chondroitin sulfates (OSCSs) exhibit this effect, and such a side effect may cause acute hypersensitivity reactions and endanger the lives of patients (28–30). Compared with **1**, low concentrations of **2** exhibited significantly reduced FXII activation, whereas high concentrations (>16 μg/mL) of **2** and **8** still activated FXII. However, no FXII activation was observed when **3**–**7** were tested within the experimental concentration range (Fig. 4*B* and *SI Appendix*, S9*D*). Regarding platelet aggregation, **1** (30 μg/mL) significantly induced aggregation (68.3 ± 7.9%, $P < 0.001$ vs. control); however, **2**–**8** (30 μg/mL) exhibited no obvious platelet aggregation (9.8 ± 6.0%, $P > 0.05$ vs. control) (Fig. 4*C*).

Compound 5 Exhibits High Antithrombotic Activity and Less Bleeding in Vivo. Our data suggest that **5**–**7** exhibit strong in vitro anticoagulant activities by selectively inhibiting human intrinsic tenase and have negligible side effects, such as the activation of human FXII and the induction of platelet aggregation. Our results also reveal that at least three trisaccharide repeating units are required both for the strong intrinsic anticoagulant activity and for the potent selective inhibition of the intrinsic tenase. Therefore, we further determined the antithrombotic activity and bleeding risk of **5** in vivo.

In the venous thrombosis model, **5** exhibited strong inhibition of venous thrombus formation with thrombosis inhibition rates of 67.2% and 97.4% at doses of 5 and 10 mg/kg, respectively. The thrombosis inhibition rate of LMWH was 96.7% at 3.6 mg/kg (Fig. 5*A*). It is known that the inhibition of thrombus formation of LMWH is mainly related to inhibition of FXa mediated by AT (1). In this study, based on the results of coagulation (co)factor assays (Fig. 4 and Table 1), the antithrombotic efficacy of **5** is attributed to selective inhibition of the intrinsic tenase.

Next, we evaluated the effect of **5** on blood loss in mouse models (Fig. 5*B*). Compared with the blood loss in the normal control group, LMWH significantly increased blood loss at a dose of 42 mg/kg ($P < 0.05$). In contrast, **5** had no obvious effect at doses of 60 and 120 mg/kg ($P > 0.05$) (Fig. 5*B*). These results suggest that targeting the intrinsic tenase via the AT-independent inhibition mechanism may improve the risk/benefit ratio of antithrombotic therapy. Additionally, medicinal properties in vivo of other promising compounds such as **6** and **7** may also be distinct and worthy of further elucidation in the future.

Discussion

FG, a novel glycosaminoglycan derivate from sea cucumber, is markedly different from typical mammalian glycosaminoglycans, such as dermatan sulfate and chondroitin sulfate, because of its unique sulfated fucose side chains, although it possesses a chondroitin sulfate-like backbone (31). In recent years, FG has attracted increasing attention from researchers because of its high yields (~1%) from the dried body wall of sea cucumber and because of its biological activities, including anticoagulant, antithrombotic, anticancer, and anti-HIV activities (14, 31–33). Over the past 30 y, the basic structure of FG has been studied using chemical methods such as desulfation, defucosylation, and methylation together with NMR analyses and analyses of the products formed by digesting the partially defucosylated chondroitin sulfate with chondroitinase AC or ABC (20–22). However, its detailed structures have not yet been elucidated. In this study, the structure of **1** was unequivocally established by combining the structures of a range of prepared pure fragments, and this structure shows that the Fuc side chain only exists as a monosaccharide and only attaches to GlcA in an α1,3 manner, the di- or trisaccharide side chain is absent, and no Fuc side chain links to GalNAc (or anTal-ol). These findings may be useful for elucidating the structure of other glycosaminoglycans, including FG from other sea cucumber species, and for elucidating the structure–activity relationship of FG.

Unfractionated heparin and LMWH have several limitations, such as the potential risk of contamination and serious bleeding (29, 34, 35). In recent decades, anticoagulants that have emerged as alternatives to heparin-like drugs primarily target FIIa and FXa in the common pathway of the coagulation cascade but still exhibit adverse effects, particularly the risk of serious bleeding (5, 6, 36–38). A series of studies has demonstrated that inhibitors of the activated coagulation factors in the intrinsic pathway, such as factors FIXa, FXIa, and FXIIa, should effectively prevent thrombus formation with negligible bleeding risk (8, 10, 11, 39). The intrinsic tenase is the final and rate-limiting enzyme complex in the intrinsic pathway. However, to date, no selective inhibitors of this enzyme complex have been developed. As mentioned above, FG exhibits potent anticoagulation by inhibiting this enzyme complex, but the native FG and its depolymerized products are heterogeneous and have side effects. Through preparing various oligosaccharide fragments of FG, we found that compounds **5**–**7** may be desirable intrinsic tenase inhibitors because of their relatively low molecular weights, potent intrinsic anticoagulant activity, and negligible side effects. Notably, just as a pentasaccharide unit is the critical sequence within heparin chains required to bind and activate AT (40–43), the nonasaccharide **5** is the minimum structural unit responsible for inhibiting human intrinsic tenase. The results of the antithrombotic assay show that compound **5** at 10 mg/kg has a similar antithrombotic effect as LMWH at 3.6 mg/kg. At ~12-fold the dose required for the inhibition of venous thrombosis, the blood loss of the mice increased significantly ($P < 0.05$) in the LMWH administration group compared with those of the mice in the normal control group; however, no significant difference ($P > 0.05$) was observed

Table 1. Anticoagulant activities of 1–8 and their effects on coagulation factors and cofactors

Compound	APTT,* μg/mL	TT,* μg/mL	PT,* μg/mL	Anti-tenase,† ng/mL	Anti-FXa (by AT),† ng/mL	Anti-FIIa (by AT),† ng/mL
1	1.79 ± 0.03	8~16	>128	8.9 ± 0.8	>2,000	275.5 ± 17.8
2	4.00 ± 0.21	>128	>128	11.4 ± 0.6	>2,000	>2,000
8	3.08 ± 0.06	>128	>128	11.2 ± 1.0	>2,000	1,715 ± 29
7	5.56 ± 0.14	>128	>128	13.2 ± 1.3	>2,000	>2,000
6	8.71 ± 0.12	>128	>128	55.4 ± 7.1	>2,000	>2,000
5	14.49 ± 0.06	>128	>128	103.3 ± 12.7	>2,000	>2,000
4	61.76 ± 1.80	>128	>128	>2,000	>2,000	>2,000
3	>128	>128	>128	>2,000	>2,000	>2,000
LMWH	14.82 ± 0.29	4~8	>128	97.7 ± 12.4	26.3 ± 1.2	53.5 ± 2.4

$n = 3$.

*The activity of agents to prolong APTT, PT, or TT is expressed by the concentration of each agent (μg/mL) that is required to double the APTT, PT, or TT.

†EC_{50} value, the concentration of each agent required to inhibit 50% of protease activity.

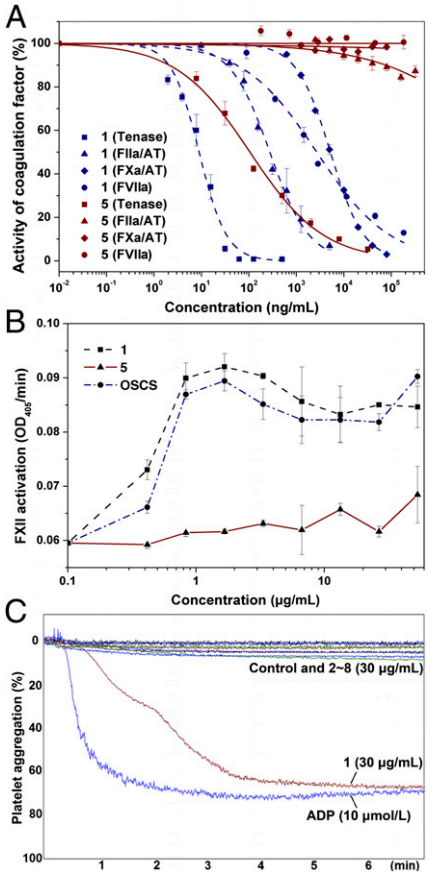

Fig. 4. Effects of **1** and **5** on intrinsic tenase activity and FVIIa, FXa, and FIIa activities in the presence of AT (*A*), FXII activation (*B*), and platelet aggregation (*C*). The results were expressed as mean ± SD (n = 3) in *A* and *B*. See Table 1 for EC_{50} values.

for the blood loss of the mice treated with **5** compared with the normal control group. These results indicate that the intrinsic tenase inhibitor may be a novel promising anticoagulant with negligible bleeding risks.

Materials and Methods

Preparation and Characterization of Oligosaccharides from FG. The native FG (HPLC purity 99.9%; average molecular mass 70 kDa) (**1**; Fig. 2*A*) was isolated and purified from the sea cucumber *S. variegatus* as previously described (24, 31). Depolymerized **1** (i.e., **2**) with an anTal-ol terminal was prepared via the partial deacetylation–deaminative cleavage of **1** as previously described (17). **2** was size-separated by GPC with Bio-Gel P6 and P10 columns (Bio-Rad Laboratories) combined with analysis using a Superdex Peptide 10/300 GL column (GE Healthcare Life Sciences) and desalted by GPC on a Bio-Gel P2 column. The purity of the oligosaccharides was determined by HPLC using a Superdex Peptide 10/300 GL column. NMR analyses of **1**–**8** were performed in D_2O on Bruker AVANCE 600- or 800-MHz spectrometers. Negative-ion ESI-MS was performed on a Bruker micrOTOF-Q II mass spectrometer. Infrared spectra were recorded on a Bruker Tensor 27 infrared spectrometer.

Anticoagulant Assays and Inhibition of the Intrinsic Tenase in the Presence of 1–8. The APTT, PT, and TT of **1**–**8**, LMWH, and dermatan sulfate (DS) were determined using assay kits on a coagulometer (TECO; MC-4000) as described previously (44). The inhibition of the intrinsic tenase was determined using the previously described method (31, 45) with modifications and the reagents in the BIOPHEN FVIII:C Kit (HYPHEN BioMed).

Effects of 1–8 on Coagulation (Co)Factors. FVIIa inhibition assays were performed according to the manufacturer's recommended procedures with modifications using assay kits (BIOPHEN FVII); inhibition assays of FIXa, FXIa, and FXIIa were measured using a Bio-Tek microplate reader. Inhibition of human FIIa in the presence of HCII was measured with the thrombin chromogenic substrate CS-01 (38). The anti-FIIa and anti-FXa activities in the presence of AT were measured using BIOPHEN Heparin Anti-FIIa Kits and Heparin Anti-FXa Kits, respectively.

Activation of Human FXII and Platelet Aggregation Assays. The activation of human FXII in the presence of samples of **1**–**8** was assessed using a previously described method (31, 46). Turbidimetric measurements of platelet aggregation by **1**–**8** were performed using a Chrono-log 700 aggregometer according to Born's method (31, 47). Venous blood from a young healthy volunteer (a 26-y-old male, ∼65 kg) was anticoagulated with 3.8% (wt/wt) sodium citrate. All procedures were approved by the Research Ethics Committee of the Kunming Institute of Botany, Chinese Academy of Sciences. The study subject provided written informed consent for the blood donation protocol obtained according to the principles of Helsinki.

Inhibition of Thrombus Formation. Antithrombotic activity was investigated in male Sprague–Dawley rats (body weight 250–300 g) from Kunming Medical University with the tissue thromboplastin-induced venous thrombosis model. The inhibition of thrombus formation in the presence of samples was determined using a previously described method with modifications (18, 31). Animal experiments were conducted according to the current ethical regulations for animal care and use and were reviewed and approved by the Animal Ethics Committee of Kunming Institute of Botany, Chinese Academy of Sciences.

Bleeding Effects. Different doses of samples were injected dorsally and s.c. into Kunming mice (body weight 18–22 g) from Kunming Medical University. After 60 min, the tails of the mice were cut 5 mm from the tip and immersed in 40 mL of distilled water for 90 min at 37 °C with stirring. Blood loss was determined by measuring the hemoglobin present in the water using a spectrophotometric method (48). The volume of blood was determined from a standard curve based on absorbance at 540 nm.

Statistical Analysis. The data were analyzed using one-way analysis of variance (ANOVA) followed by Duncan's multiple-range test (DMRT) using IBM SPSS statistics version 19.0. All values for each group were given as the means ± SD. P values less than 0.05, 0.01, or 0.001 were considered to be statistically significant (i.e., $*P < 0.05$, $**P < 0.01$, or $***P < 0.001$).

A full description of the materials and methods can be found in *SI Appendix, SI Materials and Methods*.

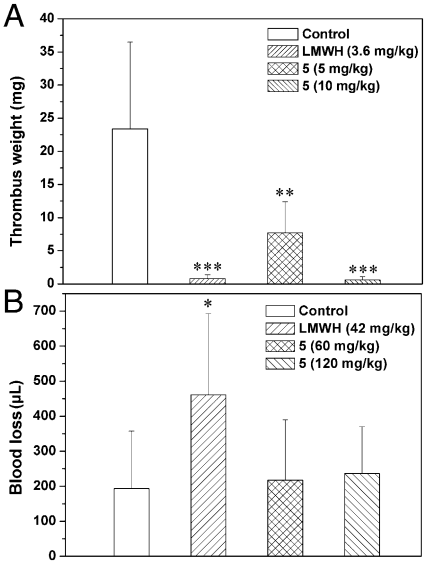

Fig. 5. Venous antithrombotic activity (*A*) and bleeding effect (*B*) of **5** in vivo. Antithrombotic activity was investigated in male Sprague–Dawley rats with the tissue thromboplastin-induced venous thrombosis model. The results are expressed as thrombus weight (mean ± SD, $n = 8$, $**P < 0.01$, $***P < 0.001$ vs. control). (*B*) Different doses of compounds were infused into mice. Blood loss was determined by measuring the hemoglobin present in the water using a spectrophotometric method. The results were expressed as microliters of blood loss (mean ± SD, $n = 6$, $*P < 0.05$ vs. control).

ACKNOWLEDGMENTS. We thank Prof. K. F. Hu, Dr. X. H. Shi, and Dr. B. Li for performing the NMR experiments. This work was funded in part by the Yunnan Provincial Science and Technology Department in China (2010CI116, 2013FA046, and 2012FB177), National Natural Science Foundation of China (81102372 and 81373292), Outstanding Technical Talent Foundation, and West Light Foundation of the Chinese Academy of Sciences.

1. Mackman N (2008) Triggers, targets and treatments for thrombosis. *Nature* 451(7181): 914–918.
2. Lee AYY, et al.; Randomized Comparison of Low-Molecular-Weight Heparin Versus Oral Anticoagulant Therapy for the Prevention of Recurrent Venous Thromboembolism in Patients with Cancer (CLOT) Investigators (2003) Low-molecular-weight heparin versus a coumarin for the prevention of recurrent venous thromboembolism in patients with cancer. *N Engl J Med* 349(2):146–153.
3. Liu J, Linhardt RJ (2014) Chemoenzymatic synthesis of heparan sulfate and heparin. *Nat Prod Rep* 31(12):1676–1685.
4. Waxman L, Smith DE, Arcuri KE, Vlasuk GP (1990) Tick anticoagulant peptide (TAP) is a novel inhibitor of blood coagulation factor Xa. *Science* 248(4955):593–596.
5. Lassen MR, et al.; ADVANCE-3 Investigators (2010) Apixaban versus enoxaparin for thromboprophylaxis after hip replacement. *N Engl J Med* 363(26):2487–2498.
6. Cohen AT, et al.; MAGELLAN Investigators (2013) Rivaroxaban for thromboprophylaxis in acutely ill medical patients. *N Engl J Med* 368(6):513–523.
7. Schulman S, et al.; RE-COVER II Trial Investigators (2014) Treatment of acute venous thromboembolism with dabigatran or warfarin and pooled analysis. *Circulation* 129(7):764–772.
8. Matafonov A, et al. (2014) Factor XII inhibition reduces thrombus formation in a primate thrombosis model. *Blood* 123(11):1739–1746.
9. Carmeliet P (2001) Biomedicine. Clotting factors build blood vessels. *Science* 293(5535):1602–1604.
10. Eikelboom JW, Zelenkofske SL, Rusconi CP (2010) Coagulation factor IXa as a target for treatment and prophylaxis of venous thromboembolism. *Arterioscler Thromb Vasc Biol* 30(3):382–387.
11. Younis HS, et al. (2012) Antisense inhibition of coagulation factor XI prolongs APTT without increased bleeding risk in cynomolgus monkeys. *Blood* 119(10):2401–2408.
12. Mann KG, Nesheim ME, Church WR, Haley P, Krishnaswamy S (1990) Surface-dependent reactions of the vitamin K-dependent enzyme complexes. *Blood* 76(1):1–16.
13. Brandstetter H, Bauer M, Huber R, Lollar P, Bode W (1995) X-ray structure of clotting factor IXa: Active site and module structure related to Xase activity and hemophilia B. *Proc Natl Acad Sci USA* 92(21):9796–9800.
14. Pomin VH (2014) Holothurian fucosylated chondroitin sulfate. *Mar Drugs* 12(1): 232–254.
15. Nagase H, et al. (1995) Depolymerized holothurian glycosaminoglycan with novel anticoagulant actions: Antithrombin III- and heparin cofactor II-independent inhibition of factor X activation by factor IXa-factor VIIIa complex and heparin cofactor II-dependent inhibition of thrombin. *Blood* 85(6):1527–1534.
16. Buyue Y, Sheehan JP (2009) Fucosylated chondroitin sulfate inhibits plasma thrombin generation via targeting of the factor IXa heparin-binding exosite. *Blood* 114(14): 3092–3100.
17. Zhao L, et al. (2013) Structure and anticoagulant activity of fucosylated glycosaminoglycan degraded by deaminative cleavage. *Carbohydr Polym* 98(2):1514–1523.
18. Fonseca RJC, et al. (2010) Effects of oversulfated and fucosylated chondroitin sulfates on coagulation. Challenges for the study of anticoagulant polysaccharides. *Thromb Haemost* 103(5):994–1004.
19. Kitazato K, Kitazato KT, Nagase H, Minamiguchi K (1996) DHG, a new depolymerized holothurian glycosaminoglycan, exerts an antithrombotic effect with less bleeding than unfractionated or low molecular weight heparin, in rats. *Thromb Res* 84(2): 111–120.
20. Panagos CG, et al. (2014) Fucosylated chondroitin sulfates from the body wall of the sea cucumber *Holothuria forskali*: Conformation, selectin binding, and biological activity. *J Biol Chem* 289(41):28284–28298.
21. Vieira RP, Mourão PAS (1988) Occurrence of a unique fucose-branched chondroitin sulfate in the body wall of a sea cucumber. *J Biol Chem* 263(34):18176–18183.
22. Kariya Y, Watabe S, Hashimoto K, Yoshida K (1990) Occurrence of chondroitin sulfate E in glycosaminoglycan isolated from the body wall of sea cucumber *Stichopus japonicus*. *J Biol Chem* 265(9):5081–5085.
23. Mourão PAS, et al. (1996) Structure and anticoagulant activity of a fucosylated chondroitin sulfate from echinoderm. Sulfated fucose branches on the polysaccharide account for its high anticoagulant action. *J Biol Chem* 271(39):23973–23984.
24. Wu M, Xu S, Zhao J, Kang H, Ding H (2010) Physicochemical characteristics and anticoagulant activities of low molecular weight fractions by free-radical depoly merization of a fucosylated chondroitin sulphate from sea cucumber *Thelenata ananas*. *Food Chem* 122(3):716–723.
25. Yang J, et al. (2015) Depolymerized glycosaminoglycan and its anticoagulant activities from sea cucumber *Apostichopus japonicus*. *Int J Biol Macromol* 72:699–705.
26. Chi L, et al. (2008) Structural analysis of bikunin glycosaminoglycan. *J Am Chem Soc* 130(8):2617–2625.
27. Al-Horani RA, Ponnusamy P, Mehta AY, Gailani D, Desai UR (2013) Sulfated pentagalloylglucoside is a potent, allosteric, and selective inhibitor of factor XIa. *J Med Chem* 56(3):867–878.
28. Kishimoto TK, et al. (2008) Contaminated heparin associated with adverse clinical events and activation of the contact system. *N Engl J Med* 358(23):2457–2467.
29. Guerrini M, et al. (2009) Orthogonal analytical approaches to detect potential contaminants in heparin. *Proc Natl Acad Sci USA* 106(40):16956–16961.
30. Kalita M, et al. (2014) A nanosensor for ultrasensitive detection of oversulfated chondroitin sulfate contaminant in heparin. *J Am Chem Soc* 136(2):554–557.
31. Wu M, et al. (2015) Anticoagulant and antithrombotic evaluation of native fucosylated chondroitin sulfates and their derivatives as selective inhibitors of intrinsic factor Xase. *Eur J Med Chem* 92:257–269.
32. Wu M, Xu S, Zhao J, Kang H, Ding H (2010) Free-radical depolymerization of glycosaminoglycan from sea cucumber *Thelenata ananas* by hydrogen peroxide and copper ions. *Carbohydr Polym* 80(4):1116–1124.
33. Lian W, et al. (2013) Anti-HIV-1 activity and structure-activity-relationship study of a fucosylated glycosaminoglycan from an echinoderm by targeting the conserved CD4 induced epitope. *Biochim Biophys Acta* 1830(10):4681–4691.
34. Nugent MA (2000) Heparin sequencing brings structure to the function of complex oligosaccharides. *Proc Natl Acad Sci USA* 97(19):10301–10303.
35. Milovic NM, et al. (2006) Monitoring of heparin and its low-molecular-weight analogs by silicon field effect. *Proc Natl Acad Sci USA* 103(36):13374–13379.
36. Crowther MA, Warkentin TE (2008) Bleeding risk and the management of bleeding complications in patients undergoing anticoagulant therapy: Focus on new anticoagulant agents. *Blood* 111(10):4871–4879.
37. Goldhaber SZ, et al.; ADOPT Trial Investigators (2011) Apixaban versus enoxaparin for thromboprophylaxis in medically ill patients. *N Engl J Med* 365(23):2167–2177.
38. Oh YI, Sheng GJ, Chang S-K, Hsieh-Wilson LC (2013) Tailored glycopolymers as anticoagulant heparin mimetics. *Angew Chem Int Ed Engl* 52(45):11796–11799.
39. MacQuarrie JL, et al. (2011) Histidine-rich glycoprotein binds factor XIIa with high affinity and inhibits contact-initiated coagulation. *Blood* 117(15):4134–4141.
40. Petitou M, van Boeckel CAA (2004) A synthetic antithrombin III binding pentasaccharide is now a drug! What comes next? *Angew Chem Int Ed Engl* 43(24): 3118–3133.
41. Polat T, Wong CH (2007) Anomeric reactivity-based one-pot synthesis of heparin-like oligosaccharides. *J Am Chem Soc* 129(42):12795–12800.
42. Xu Y, et al. (2011) Chemoenzymatic synthesis of homogeneous ultralow molecular weight heparins. *Science* 334(6055):498–501.
43. Chang CH, et al. (2014) Synthesis of the heparin-based anticoagulant drug fondaparinux. *Angew Chem Int Ed Engl* 53(37):9876–9879.
44. Gao N, et al. (2012) Preparation and characterization of O-acylated fucosylated chondroitin sulfate from sea cucumber. *Mar Drugs* 10(8):1647–1661.
45. Sheehan JP, Walke EN (2006) Depolymerized holothurian glycosaminoglycan and heparin inhibit the intrinsic tenase complex by a common antithrombin-independent mechanism. *Blood* 107(10):3876–3882.
46. Hojima Y, Cochrane CG, Wiggins RC, Austen KF, Stevens RL (1984) In vitro activation of the contact (Hageman factor) system of plasma by heparin and chondroitin sulfate E. *Blood* 63(6):1453–1459.
47. Born GVR (1962) Aggregation of blood platelets by adenosine diphosphate and its reversal. *Nature* 194(4832):927–929.
48. Pacheco RG, Vicente CP, Zancan P, Mourão PA (2000) Different antithrombotic mechanisms among glycosaminoglycans revealed with a new fucosylated chondroitin sulfate from an echinoderm. *Blood Coagul Fibrinolysis* 11(6):563–573.